Economic Dynamics of Epidemiological Bifurcations

David Aadland, David Finnoff and Kevin X.D. Huang*

September 2018

Abstract

In this paper, we investigate the nature of rational expectations equilibria for economic epidemiological models, with a particular focus on the behavioral origins and dynamics of epidemiological bifurcations. Unlike mathematical epidemiological models, economic epidemiological models can produce regions of indeterminacy or instability around the endemic steady states due to endogenous human responses to epidemiological circumstance variation, medical technology change, or health policy reform. We consider SI, SIS, SIR and SIRS versions of economic compartmental models and show how well-intentioned public policy may contribute to disease instability, uncertainty, and welfare losses.

JEL Codes: D1, I1.

Keywords: economic epidemiology, bifurcation, endogenous disease risk, rational expectations, dynamic optimal decision, public policy, aggregate instability, indeterminacy, sunspots, self-fulfilling prophecies, welfare loss

1 Introduction

In this paper we investigate the dynamics of epidemiological bifurcations in systems where individuals optimally alter behavior in the face of endogenous disease risk.[1] The bifurcations can lead to aggregate instability, which introduces the potential for less predictable outcomes from public health policies and welfare losses. For instance, health policies designed to lower the transmission probability (e.g., public screening, rapid diagnostic services, and prescriptions of preventative therapies) or policies designed to raise the quality-of-life following infection (e.g., public provisioning of curative therapies) by generating endogenous human responses may push endemic equilibria from being stable to exhibiting instability or indeterminacy. The latter also have the potential of contributing to "sunspot" equilibria, which have been considered in dynamic macroeconomic models and contribute to the volatility and unpredictability of the system (e.g., Grandmont (1986); Woodford (1986); Smith (1989); Benhabib and Farmer (1999); Farmer (1999); Farmer (2010)). The amount of attention paid to potential extrinsic instability and welfare reduction induced by monetary or fiscal policy in the face of optimal human behavior is quite remarkable, see, among many others: Guo and Lansing (2002); Xiao (2008); Huang and Meng (2009); Huang, Meng, and Xue (2009); Anagnostopoulos and Giannitsarou (2013); Guo and Krause (2014); and Abad, Seegmuller, and Venditti (2017). Perhaps equally remarkable is the lack of attention to such potential problems associated with health policy. The present paper fills this void. Our results suggest that the design or operation of public health policy must recognize that it may constitute a source of self-fulfilling prophecies and extrinsic uncertainty in the face of rational agents making optimal choices. We also show how the observability of an SIRS disease status leads to a type of dynamic externality imposed on the economic system that differs from the infection externality typically stressed in the literature (e.g., Kremer (1996); Gersovitz and Hammer (2004)).

The potential for epidemiological bifurcations in discrete time compartmental models are well known[2], but their connection to social interactions and human behavioral responses are less well documented (other than in Aadland, Finnoff, and Huang (2013)). Feng, Castillo-Chavez, and Capurro (2000) demonstrate a bifurcation in endemic equilibria of an SIS model of tuberculosis, taking the per person contact rate as constant. Variation in the contact rate has been shown to lead to a variety of dynamic possibilities (e.g., van den Driessche and Watmough (2000); Dodds and Watts (2005)). Dodds and Watts demonstrate

---

[1] By epidemiological bifurcations, we are referring to the general idea that "...the state of the [epidemiological] system depends on some parameter .... usually with a concomitant change in stability" Shivamoggi (2014).

[2] Discrete time systems have been shown (e.g., Allen (1994)) to have endemic equilibria that are stable, periodic or chaotic depending on magnitude of contact rates and birth/death rates. How the contact rates vary depending upon the epidemiological state of the system is typically omitted (i.e., human behavior does not change as epidemiological circumstance change). Continuous-time epidemiological systems (e.g., Korobeinikov and Wake (2002)), in contrast, typically find a single endemic equilibrium that is globally stable.

the influence of alternative exposure mechanisms on dynamics of epidemiological systems, while van den Driessche and Watmough investigate the impact of a non-constant contact rate. Both studies find a deep set of dynamic possibilities including multiple equilibria, bifurcations and hysteresis.

The framework developed in this paper provide a behavioral rationale that underlies many of the models in the mathematical epidemiological literature. A foundation of intertemporal human behavioral responses to changing epidemiological conditions, medical technologies, and health policies causes interdependent exposures and non-constant contact rates, which in turn leads to dynamic complexity and the possibility of unintended welfare consequences from public health policy.

2 An Epidemiological Model with Human Response

Following work by Philipson and Posner (1993) and Lightwood and Goldman (1995), we specify an integrated epidemiological model to describe individual behavior in the face of endogenous risk of infection from a communicable disease. In any period t, individual i from a constant population of N individuals[3] is in one of three epidemiological states as indicated by the binary variables: susceptible ($s_{i,t}$), infected ($in_{i,t}$), or recovered and immune ($r_{i,t}$). The proportions of susceptible, infected and recovered individuals in the entire population are given by averaging over all i.[4] A similar model is presented in Aadland, Finnoff, and Huang (2013) to examine the dynamics and potential eradication of syphilis.

The risk of infection is endogenous because individuals choose to engage in activities which affect their exposure to the disease. Additional exposure brings immediate satisfaction but also the risk of future infection, leading to a deterioration of the individual's health. We assume current utility of an individual depends on their choice of exposure in a period, $x_{i,t}$, and their health status $h_{i,t}$. As exposure is a direct choice and health status an indirect consequence of past choices, we assume utility is diminishing in exposure and linear in health status. Individuals maximize expected lifetime utility by choosing exposure in each period

$$\max_{\{x_{i,t}\}} E_t \sum_{j=0}^{\infty} \beta^j [\ln(x_{i,t+j}) + h_{i,t+j}] \tag{1}$$

where $0 < \beta < 1$ is the discount factor, E_t represents an individual's rational expectation of future outcomes conditional on all information dated t and earlier, $\bar{x}$ is the maximum feasible amount of exposure per period. For tractability, we assume the health status of individuals in each epidemiological state is constant and

---

[3] See Derrick and Van Den Driessche (1993) for an example of a disease transmission model with a non-constant population.
[4] The model is set in discrete time (e.g., Allen (1994), Auld (2003), Lightwood and Goldman (1995)), where t indexes the decision interval.

the health status of susceptible (or recovered/immune) individuals exceeds that of infected individuals, $h^S > h^{IN}$. All individuals maximize (1) without concern for the welfare of the general population, subject to the epidemiological dynamics.

2.1 Epidemiology

The epidemiological portion of the model describes the evolution of the three mutually exclusive disease categories measured as proportions of the overall population. We specify the most general SIRS model (e.g., Anderson and May (1991)), where individuals transition from being susceptible to infected to recovered (and immune) and then back to susceptible. The SIRS model has previously been used to model infectious diseases such as syphilis and whooping cough (e.g., Grassly, Fraser, and Garnett (2005); Rohani, Zhong, and King (2010)). The SIRS model is sufficiently general to handle cases with permanent infection (SI diseases such as HIV/AIDS), diseases with recovery but no immunity (SIS diseases such as the common cold and active tuberculosis), and diseases with permanent immunity (SIR diseases such as measles and chicken pox).

The disease dynamics are represented by the system

$$s_{t+1} \;=\; \mu + (1 - p_t - \mu)s_t + \gamma r_t \tag{2}$$

$$in_{t+1} \;=\; (1 - v - \mu)in_t + p_t s_t \tag{3}$$

$$r_{t+1} \;=\; (1 - \gamma - \mu)r_t + v\,in_t, \tag{4}$$

where μ is the common birth/death rate, $1/\gamma$ is the average duration of immunity, v is the recovery rate, and p_t is the probability of infection for a susceptible individual, which depends on prevalence in_t and their exposure choices, $x_{i,t}$. If the disease is transmitted person-to-person such as an STD, then $x_{i,t}$ can be interpreted as the chosen number of partners. If the disease is vector-borne such as the common cold, measles or malaria, then $x_{i,t}$ can be interpreted as exposure time to the disease. Assuming independence across episodes of exposure, the probability that (identical) susceptible individuals become infected is given by

$$p_t = \Pr(\text{infection}) = 1 - (1 - \lambda in_t)^{x_{i,t}}, \tag{5}$$

where λ is the per unit exposure (or per partner) transmission rate (e.g., Dodds and Watts (2005),Kaplan (1990); Oster (2005)).

4

Imposing the condition that all three categories sum to one, the disease dynamics simplify to:

$$in_{t+1} = (1 - p_t - v - \mu)in_t + p_t(1 - r_t) \tag{6}$$

$$r_{t+1} = (1 - \gamma - \mu)r_t + vin_t, \tag{7}$$

where p_t is given by (5). The SIR model sets $\gamma = 0$ so that individuals are permanently recovered and immune to the disease. The SIS and SI models omit the immunity category.

2.2 Decision Making

The value functions for each state – susceptible (S), infected (IN), and recovered (R) – are given by

$$V_t^S = \ln(x_t) + h^S + \beta E_t[p_t V_{t+1}^{IN} + (1 - p_t)V_{t+1}^S] \tag{8}$$

$$V_t^{IN} = \ln(\bar{x}) + h^{IN} + \beta E_t[v V_{t+1}^R + (1 - v)V_{t+1}^{IN}] \tag{9}$$

$$V_t^R = \ln(\bar{x}) + h^S + \beta E_t[\gamma V_{t+1}^S + (1 - \gamma)V_{t+1}^R], \tag{10}$$

where infected and immune individuals choose the maximum feasible amount of exposure, $\bar{x}$, because they face no risk of immediate infection (e.g., Geoffard and Philipson (1996)). Similar to Gersovitz and Hammer (2004), this behavior imposes an externality on susceptible individuals. We discuss this in detail later in the paper. In contrast, susceptible individuals will choose the degree of exposure that balances the current marginal benefits of exposure with the discounted expected future marginal costs of exposure as given by the Euler equation:

$$x_t^{-1} = \beta p_{x,t} E_t[V_{t+1}^S - V_{t+1}^{IN}], \tag{11}$$

where the partial derivative of p_t with respect to the degree of exposure is $p_{x,t} = -\ln(1 - p_t)(1 - p_t)/x_{it}$.[5] The left side of (11) gives the marginal benefit of exposure, while the right side of (11) gives the expected future marginal costs of exposure. The implication from (11) is that individuals will choose to expose themselves until the marginal benefits from additional exposure cease to outweigh the marginal costs of exposure. However, unlike models where the infection rate is constant or varies mechanistically (e.g., Dodds and Watts (2005); Korobeinikov (2006)), the term $p_{x,t}$ highlights the fact that the transition probability from susceptible to infected is endogenous. Aadland, Finnoff, and Huang (2013) demonstrate the implications

---

[5] The standard sufficiency conditions for this epidemiology problem do not hold (e.g., Goenka and Liu (2012); Gersovitz and Hammer (2004)). Therefore, we use numerical simulation to check the optimality of the transition path given by equation (11).

of the decision rule in (11). While the marginal benefits of exposure diminish with additional exposure, the marginal costs of exposure rise (fall) when exposure is low (high). This curious shape follows from exposure increasing the probability of infection, putting an upward pressure on marginal costs, but as the probability rises its rate of change decreases, pushing marginal costs back down. At low levels of exposure the former effect overwhelms the latter effect, while the reverse occurs at high levels of exposure. This type of endogenous risk creates a non-convexity.

2.2.1 Non-Convexities and Multiple Equilibria

The implication from the non-convexity is the potential for multiple equilibria, which is well-known in economic epidemiological models (e.g., Goldman and Lightwood (2002)). What is not so well known are the dynamic consequences of the non-convexities. They cause both bifurcations in equilibria and can alter the stability properties of equilibria. Bifurcations can occur from changes in any parameter that alter the marginal benefit or cost of exposure. We focus on two parameters that are levers of public policy, the per unit transmission rate, λ, and the health status of the infected state, h^{IN}.

Consider an application of the model to active tuberculosis in a developed country (SIS, loosely based on Feng, Castillo-Chavez, and Capurro (2000)) with benchmark parameter values as shown in Table 1.

<div align="center">

Table 1. SIS Parameter Values

Parameters	β	μ	v	$\bar{x}$	λ	h^{IN}	h^S
Value	0.96	0.05	1	100	0.5	20	50

</div>

The value of β implies a 4% annual discount rate, μ gives a 5% birth and death rate for the population (e.g., Garnett et al. (1997)), recovery is complete with modern curative therapies ($v = 1$), and the maximum annual number of exposures is set at 100.

Equilibria and Stability The non-convexities and their dynamic implications are illustrated in Figures 1-3. The left panel of Figure 1a plots the steady-state marginal benefit and marginal cost curves across a range of values of λ. The range in λ reflects the potential for public health policy to reduce the per unit transmission rate, from the benchmark value of $\lambda = 0.5$ to a relatively low value of $\lambda = 0.05$. For each parameter combination there are up to two equilibria, one with a relatively low degree of exposure (equilibrium points 1, 3 and 5) and one with a relatively high degree of exposure (equilibrium points 2 and 4). Public health policies that lead to lower λ's result in a reduction in marginal costs for low exposures and an increase in marginal costs for high exposures. Policies that result in lower λ's cause increases in

exposure for both the low-exposure and high-exposure equilibria (i.e., the movements from equilibrium 1 to 3 to 5 and the movement from equilibrium 2 to 4).

In contrast, the right panel of Figure 1a considers the implications on optimal choices of a public health policy that increases the health status of the infected state (i.e., a reduction in the consequences of being infected, an increase in h^{IN} from 20 to 43). Increases in h^{IN} scale the marginal cost curve downwards. The marginal costs associated with all levels of exposure decline, yet the exposure required to attain a certain level of marginal costs increases for low exposures, and falls for high exposures. The result is a small increase in the low-exposure equilibrium (such as the movement from equilibrium 1 to 3) and a larger decrease in the high-exposure equilibrium (movement from equilibrium 2 to 4). Further increases in h^{IN} – beyond where the curves are tangent – cause the marginal benefits of exposure to be everywhere greater than the marginal costs (as seen with $h^{IN} = 43$). Here, a bifurcation occurs and the two equilibrium points merge into one, leading susceptible individuals to choose the maximum level of exposure.

Figure 1b demonstrates the bifurcations in exposure that occur for variations in λ or h^{IN} (holding the other parameters constant at the benchmark values of $\lambda = 0.5$ or $h^{IN} = 20$). The figure plots both equilibria and notes their local stability properties using the method of Blanchard and Kahn (1980). The equilibria can exhibit local saddle-path stability, indeterminate paths (infinite number of paths), or unstable explosive paths. There are significant differences implied by Figure 1b and and that presented in Feng, Castillo-Chavez, and Capurro (2000). The differences result from our model being a controlled system, where the system can be manipulated to stay on a saddle path, versus the system of Feng, Castillo-Chavez, and Capurro (2000) which is uncontrolled, making the stable, indeterminate paths the focus. In a controlled system, saddle-path stability means public intervention can play a meaningful, predictable role. Yet, in a controlled system, indeterminacy and multiple equilibrium paths (the stable region of Feng, Castillo-Chavez, and Capurro (2000)) leads to the possibility of "sunspot" equilibria (e.g., Benhabib and Farmer (1999)). Sunspot equilibria are often associated with self-fulfilling prophecies and additional aggregate volatility (e.g., Farmer (1999); Farmer (2010)). The point is that in such a region, there is not a unique optimal path. Any path will lead to the equilibrium, so paths with and without public intervention will be equivalent, significantly complicating evaluations of public intervention.

Figures 1b-d illustrate the implications of the bifurcations on individual exposure decisions, aggregate outcomes (summarized by the contact rate[6]), and equilibrium individual welfare measured by the value

---

[6]Contact rates are often defined as the average number of adequate exposures per person per unit time for the infection to be transmitted (Hethcote (2000)). In our setting, the contract rate is endogenous and given by (p/in). It summarizes changes in both the probability of tranmission and prevalence.

function of susceptible individuals (equation 8). The figures demonstrate that variations in the key policy parameters lead to significantly different equilibrium exposure levels, contact rates, susceptible value functions and a wide variety of approach paths. Reductions in λ below the benchmark value lead to increased equilibrium exposure, increased contact rates (for lower equilibrium), increased equilibrium value functions for susceptible individuals, and differing approach paths. Consider a reduction in λ from the benchmark value of $\lambda = 0.5$ to $\lambda = 0.15$, associated with a movement from equilibrium points (1,2) to (3,4). While exposure levels and susceptible value functions increase for both upper and lower equilibria, the contact rate increases for the lower equilibrium and decreases for the upper equilibrium. The reasons follow from differences in changes in prevalence and probability of transmission. The reduction in λ leads to more exposure at each equilibrium, yet while the probability of transmission increases at both equilibria, it increases at a decreasing rate for the upper equilibrium (as it approaches 1) and at an increasing rate for the lower equilibrium. The increase in exposure is high enough at the upper equilibrium to actually increase prevalence, although at the lower equilibrium prevalence falls. Together, the changes lead to the contact rates shown in Figure 1c, with lower contact rates for the upper equilibrium at low λ. Low contact rates are problematic as they indicate situations when transmission will occur with few contacts or exposures.

As the equilibria change, the approach paths can also vary. The approach paths at the benchmark levels are both saddle (unique) paths, but as λ is lowered, the path to the upper equilibrium switches to being indeterminate. Although the equilibrium value function is increased, the path can be volatile.

In contrast, consider a public policy that increases h^{IN} above the benchmark, as given by the movement (in the right-hand figures) from point (1,2) to (3,4). The increase in infected health status pulls the two equilibria together and the saddle paths switch to unstable spirals. While the exposure level chosen at the lower equilibrium increases, it decreases at the upper equilibrium (as shown on the right-hand panel in Figure 1a). The contact rate changes in the same direction as exposure, given the reduction in the probability of transmission and prevalence at the upper equilibrium and increase in probability and prevalence at the lower equilibrium. The increase in infected health status has little effect on the value function of a susceptible individual at the lower equilibrium, yet has a large increase on that for the upper equilibrium. Further increases in h^{IN} that approach the health status of a susceptible individual (h^S) cause the equilibria to merge and become a single unstable equilibrium where individuals choose the maximum exposure, with high contact rates, high value functions, and volatility.

Thus, public policy aimed at lowering λ or raising h^{IN} may induce indeterminacy or aggregate instability, in either case lowering the predictability of policy interventions and leading to increased fluctuations in disease

8

prevalence.

Dynamics and Welfare To consider the dynamic implications of public policies which reduce λ or increase h^{IN}, we use GAMS to solve for nonlinear transition paths as a dynamic mixed complementary problem. Figure 2 plots the transition paths for prevalence (in_t) and exposure (x_t) that correspond from changes in λ and h^{IN} from their benchmark values. Figure 3 illustrates the welfare implications of the transition paths by presenting the discounted, expected utility[7], as well as mean and standard deviation of prevalence and exposure along each path. In each panel of Figure 2, the equilibrium points of Figure 1 are shown along with the transition paths (where arrows indicate the direction of change). The parameter changes in λ and h^{IN} cause the low-exposure equilibrium to move from equilibrium (1) to (3) and the high-exposure equilibrium to move from equilibrium (2) to (4). The 45 degree lines represent time-invariant levels of each variable.

Consider a policy that reduces λ from the benchmark value of 0.5 to 0.15, as shown in panel (a) of Figure 2. Figure 1b classifies the low-exposure equilibrium in both cases as being saddle-path stable (points 1 and 3 in Figure 1), while the high-exposure equilibrium switches from a saddle path to indeterminate (points 2 and 4 in Figure 1). The nonlinear dynamics for the low-exposure equilibrium are simple – there is a small increase in equilibrium prevalence and exposure with a quick convergence from point 1 to 3. Along the transition path for the high-exposure equilibrium, the reduced per unit transmission leads to a increase in exposure (point 2 to 4), and fluctuations in exposure and prevalence as the system converges. Figure 3a demonstrates the aggregate implications. The reduction in λ leads to an increase in expected discounted welfare for both equilibrium paths, a reduction in mean prevalence (in_t), and an increase in mean exposure (x_t). The low-exposure equilibrium has higher welfare and is the preferred equilibrium. In addition, while the variability in prevalence falls for both equilibrium paths, the variability in the level of exposure along the low path declines while the variability of exposures on the high path rises. In sum, the small decline in prevalence comes with a large, less volatile increase in exposure, and welfare improves.

The dynamic implications from policies to increase the quality of life for those infected, h^{IN}, are shown in panels (b) and (c) of Figure 2. For an increase in h^{IN} from the benchmark value to a level of 40 in panel (b), both equilibria remain on the saddle paths, converging to the new equilibria. On the low-exposure path,

---

[7]For each transition path and equilibrium, aggregate measures of expected welfare are calculated as discounted utility in each health state. Aggregate welfare along each path is specified as the expected value of the discounted sum of individual utility in each health state, for the low (L) and high (H) equilibria, $k = \{L, H\}$:

$$W_k = \sum_{j=0}^{\infty} \beta^j \left\{ \left(\ln(x_{k,t+j}) + h^S \right) s_{k,t+j} + \left(\ln(\bar{x}) + h^{IN} \right) in_{k,t+j} \right\}.$$

prevalence and exposure increase. While more individuals are infected their quality of life has significantly improved and aggregate welfare increases (as shown in Figure 3b). On the high-exposure path, prevalence and exposure decrease with a similar increase in welfare. Again, the low-exposure equilibrium path is preferred. Interestingly, increasing h^{IN} further to a level high enough that the two equilibria merge into one (i.e., $h^{IN} = 0.43$) as shown in panel (c), causes individuals to choose the maximum level of exposure and the equilibrium to be unstable and have volatile (yet not very damaging) prevalence.

2.2.2 SIRS Immunity Externality

Human beliefs over diseases, or lack thereof, also lead to significant changes in behavior and dynamics of the system. This is especially clear for SIRS diseases such as pertussis or syphilis. Although these diseases have an interval of immunity that is typically known by the scientific or medical community, it is not often well known in the bulk of the population. Whether or not individuals know (or believe) they will experience an interval of immunity leads to a shift in the marginal cost of exposure. Specifically, when recovered individuals know or can observe their own immunity, they rationally choose the maximum feasible degree of exposure $\bar{x}$ and have health level h^S. Susceptible individuals under the same set of beliefs, on the other hand, choose a specific degree of exposure x_t to satisfy

$$x_t^{-1} = \beta p_{x,t} E_t \left[\ln(x_{t+1}/\bar{x}) + h + \frac{(1 - v - p_{t+1})}{x_{t+1}p_{x,t+1}} - \beta \Delta_{t+2} \right], \tag{12}$$

where

$$\Delta_{t+2} = \frac{v\gamma}{x_{t+2}p_{x,t+2}} + (1 - v - \gamma) \left[\ln\left(\frac{x_{t+2}}{\bar{x}}\right) + \frac{1 - p_{t+2}}{x_{t+2}p_{x,t+2}} \right] + (1 - \gamma) \left[h - \frac{1}{\beta x_{t+1}p_{x,t+1}} \right]$$

and $h = h^S - h^{IN}$ is the health gap between being susceptible and infected. See Appendix A for a derivation of equation (12). The term Δ_{t+2} captures the expected future personal "costs" of infection associated with acquired immunity. Because Δ_{t+2} enters the right side of (12) with a negative sign, the possibility of future immunity is a personal benefit of becoming infected. In the decentralized equilibrium considered here, immunity (if known) thus imposes an additional externality on society. The externality is dynamic and different than the infection externalities discussed in Gersovitz and Hammer (2004). Here, forward-looking susceptible individuals expose themselves to more risk when the possibility of immunity is known, because future infection also carries along the benefit of future immunity.

In contrast, if individuals do not know or believe they will have an interval of immunity (i.e., unobserved

immunity), individuals with immunity (i.e., the R state) believe they are susceptible, and susceptibles do not account for being immune in their decision making. In this case the term Δ_{t+2} is equal to zero and equation (12) can be rewritten as

$$x_t^{-1} = \beta p_{x,t} E_t \left[\ln(x_{t+1}/\bar{x}) + h + \frac{(1 - v - p_{t+1})}{x_{t+1}p_{x,t+1}} \right]. \tag{13}$$

Figure 4 demonstrates the implications of the externality. If the externality is internalized by the individual (i.e., they observe immunity) it lowers the marginal costs of exposure (similar to the effect of increasing h^{IN} in the SIS model, Figure 1a). For the sketch given, this results in the low-exposure choice increasing, and the high-exposure choice decreasing. While there remains two alternative equilibrium choices, the magnitudes are altered in different directions and to different degrees.

2.3 Complete SIRS Bifurcation and Stability Analysis

To perform a complete bifurcation and stability analysis[8], we extend the analysis to cover several variants of the models across all combinations of the policy parameters, λ and h^{IN}. Similar to Goenka, Liu, and Nguyen (2012), we note the existence of an eradication equilibrium but focus on endemic EE equilibria.[9] The analysis uses the parameter values in Table 1 and a few additional parameters for SIR and SIRS models. We consider treatable SIR and SIRS diseases with a 100% recovery rate within a year of infection (i.e., $v = 1$). Following Garnett et al. (1997), the SIRS variant is calibrated so individuals experience a five-year period of protective immunity (i.e., $\gamma = 0.2$).

Figures 5-7 summarize the stability and bifurcation of the exposure equilibria, across ranges of the per unit transmission rate, λ, and infected health, h^{IN}, for all of the SI, SIS, SIR and SIRS models. Infected health h^{IN} can be lowered by public policy that results in the discovery and introduction of drug treatments, while the per unit infection rate λ can be lowered through the introduction of vaccines or new prevention technologies. Our main findings are:

- EE models typically produce two endemic steady states. Aggregate welfare is always higher along the

---

[8] See Appendix B for the complete economic SIRS system used in the bifurcation and stability analysis.

[9] There is also an eradication steady state where $in = r = 0$, $s = 1$, and $x = \bar{x}$. For the range of parameter values we consider, the economic eradication steady state is locally unstable because susceptible individuals have no incentive to reduce the degree of exposure. More specifically, the local stability condition requires that the basic reproduction number, R_0, is less than one (Anderson and May (1991)). The basic reproduction number is defined as the number of secondary infections generated by a single infected individual in an otherwise susceptible population. For the SIRS model described above, we have $R_0 = p/(in(v + \mu))$. Using L'Hôpital's rule, this reduces to $R_0 = \lambda_p \bar{x}/(v + \mu)$, which is greater than one for all the parameter combinations considered below.

transition path to the low-exposure endemic steady state. For the SIRS model, the dynamic disease externality leads to increased risk-taking by susceptible individuals (along the transition path to the low-exposure steady state). Rational, forward-looking individuals who know that future infection will also carry a period of immunity will choose to be riskier than if they were unaware of the immunity.

- Increasing infected health status h^{IN} or reducing the per unit infection rate λ increases aggregate welfare for most model variants, yet can move the system from a unique stable equilibrium to one that exhibits aggregate instability and indeterminacy.

We now turn to more detailed analyses for each variant of the EE model.

2.3.1 Economic SI and SIS Models

Figure 5 shows the map of path types for the SI and SIS models around the low-exposure endemic steady state (left panels) and high-exposure endemic steady state (right panels). For high values of infected health h^{IN}, there is a single endemic steady state. In this case, the dynamics of the system are evaluated around the maximum feasible level of exposure, $\bar{x}$, because the marginal benefits of exposure are everywhere greater than the marginal costs. The top panels show the type of localized dynamic paths for the economic SI model with no available treatment, $v = 0$. The majority of the parameter space for the economic SI model is defined by saddle-path equilibria. For a given initial prevalence level (in_0), there is a unique initial exposure choice (x_0) that puts the system on a convergent path to the endemic steady state. All other initial exposure levels lead to divergent paths that violate non-negativity or non-explosion conditions. Because both the low-exposure and high-exposure steady states exhibit local saddle-path stability, the system has the potential to gravitate toward either steady state. The welfare contours show that, in the long run, society is better off at the low-exposure, low-prevalence steady state.[10]

The bottom panels of Figure 5 show the dynamic path types for the SIS model where infected individuals have access to perfectly effective treatment $(v = 1)$ and return to the susceptible pool after treatment. The parameter region for the low-exposure steady state is primarily a saddle-path equilibrium, but there is also an explosive region for the low-exposure steady state at high levels of h^{IN}. Public policy aimed at improving the health of infected individuals could inadvertently move the system from a stable saddle-path region to

---

[10] Total welfare is calculated at steady state using a weighted average of the value functions for the three disease types: $s \cdot V^S + in \cdot V^{IN} + r \cdot V^R$.

an explosive system with higher waves of prevalence as individuals rationally take more risk.[11]

To gain intuition for the types of dynamic paths in the economic SIS models, consider the exposure elasticity with respect to prevalence near the endemic steady state, $\kappa = \frac{\partial x_{ss}}{\partial in_{ss}} \frac{in_{ss}}{x_{ss}}$. Prevalence elasticity measures the percentage change in exposure for a one-percent change in prevalence. This elasticity is generally negative, indicating that susceptible individuals respond to the increased risk of infection by choosing less exposure.[12] For example, the prevalence elasticities for the economic SIS system depicted in the lower left panel of Figure 5 are negative and inelastic in the saddle-path region. In the explosive band (unstable spiral) the magnitude of κ (for the interior solutions) flips to being positive (an increase in prevalence leads to an increase in exposure) with elastic and inelastic magnitudes.

2.3.2 Economic SIR and SIRS Models with Observable Immunity

Figure 6 shows a similar map for the dynamic paths in SIR and SIRS models where immunity is observable. The top panels show the dynamic equilibrium types for the economic SIR model with permanent immunity, $\gamma = 0$. For all combinations of λ and h^{IN}, there is a single endemic steady state. For most of the parameter region, susceptible individuals choose the maximum level of exposure and the system is locally stable. This makes intuitive sense because susceptible individuals know that if they become infected, they can receive immediate treatment and enjoy a lifetime of disease immunity. There is a small range of indeterminacy for low levels of infected health and low levels of the infection parameter.

The lower panels show the path types for the economic SIRS model with $\gamma = 0.2$ (i.e., average immunity duration of five years). Unlike the economic SIR model, the economic SIRS model produces large regions of indeterminacy where there are multiple approach paths and the possibility of "sunspot" equilibria (e.g., Benhabib and Farmer (1999)). Considering that welfare is higher in the lower left panel, public policy aimed at improving the quality of life for individuals infected with diseases that have known temporary immunity may induce aggregate instability and indeterminacy.

2.3.3 Economic SIR and SIRS Models with Unobservable Immunity

Figure 7 depicts the SIRS counterpart to Figure 6 but with unobservable immunity. Unobservable immunity causes two primary changes. First, individuals in the economic SIR system now choose less exposure for any parameter combination. Knowledge of perfectly effective treatment and permanent immunity, as depicted

---

[11]Mathematical epidemiological models, by contrast, do not vary the exposure rate in response to changes in disease prevalence. For reasonable rates of exposure, the mathematical SI and SIS models are characterized by stable dynamic paths.

[12]Kremer (1996) discusses the possibility of a positive prevalence elasticity and fatalistic behavior.

in Figure 6, greatly reduces the future cost of current risky behavior. Second, the indeterminacy region for the SIRS system now covers a much smaller range of the health parameter. While well-intentioned public policy that improves the quality of life for infected individuals leads to equilibria with higher welfare, indeterminate paths that approach the equilibrium with spiral trajectories imply aggregate volatility and potentially wide swings in prevalence.

3   Conclusions

Economic epidemiology has made significant advances in educating health officials about the behavioral implications of public policies. However, one area that has received little attention is how policy and human responses influences the nature of communicable disease dynamics. In this paper, we explore the nature of the dynamics for rational expectation economic epidemiological systems. The analysis digs beneath a comparison of fixed parameter values and demonstrates the behavioral origin for epidemiological bifurcations. Indeed, we show that well-intentioned policy has the potential to create instability and indeterminacy when individuals behave rationally and in a self-interested manner. Future research should focus on providing precise policy recommendations by considering the costs of policy and applying the methods outlined in this paper to specific diseases.

References

AADLAND, D., D. FINNOFF, AND K. HUANG (2013): "Syphilis Cycles," *The B.E. Journal of Economic Analysis and Policy*, 14, 297–348.

ABAD, N., T. SEEGMULLER, AND A. VENDITTI (2017): "Nonseparable preferences do not rule out aggregate instability under balanced-budget rules: a note," *Macroeconomic Dynamics*, 21(1), 259–277.

ALLEN, L. (1994): "Some discrete-time SI, SIR, and SIS epidemic models," *Mathematical biosciences*, 124(1), 83–105.

ANAGNOSTOPOULOS, A., AND C. GIANNITSAROU (2013): "Indeterminacy and period length under balanced budget rules," *Macroeconomic Dynamics*, 17(4), 898–919.

ANDERSON, R., AND R. MAY (1991): *Infectious Diseases of Humans, Dynamics and Control.* Oxford University Press.

AULD, M. (2003): "Choices, beliefs, and infections disease dynamics," *Journal of Health Economics*, 22, 361–377.

BENHABIB, J., AND R. FARMER (1999): "Indeterminacy and sunspots in macroeconomics," *Handbook of macroeconomics*, 1, 387–448.

BLANCHARD, O. J., AND C. M. KAHN (1980): "The solution of linear difference models under rational expectations," *Econometrica*, 48(5), 1305–1311.

DERRICK, W., AND P. VAN DEN DRIESSCHE (1993): "A disease transmission model in a nonconstant population," *Journal of Mathematical Biology*, 31(5), 495–512.

DODDS, P. S., AND D. J. WATTS (2005): "A generalized model of social and biological contagion," *Journal of theoretical biology*, 232(4), 587–604.

FARMER, R. E. (1999): *The macroeconomics of self-fulfilling prophecies*. mit Press.

———— (2010): *How the economy works: confidence, crashes and self-fulfilling prophecies*. Oxford University Press.

FENG, Z., C. CASTILLO-CHAVEZ, AND A. F. CAPURRO (2000): "A model for tuberculosis with exogenous reinfection," *Theoretical population biology*, 57(3), 235–247.

GARNETT, G., ET AL. (1997): "The Natural History of Syphilis: Implications for the Transition Dynamics and Control of Infection," *Sexually Transmitted Diseases*, 24(4), 185–200.

GEOFFARD, P., AND T. PHILIPSON (1996): "Rational epidemics and their public control," *International Economic Review*, 37(3), 603–624.

GERSOVITZ, M., AND J. HAMMER (2004): "The Economical Control of Infectious Diseases," *The Economic Journal*, 114, 1–27.

GOENKA, A., AND L. LIU (2012): "Infectious diseases and endogenous fluctuations," *Economic Theory*, 50(1), 125–149.

GOENKA, A., L. LIU, AND M.-H. NGUYEN (2012): "Infectious Diseases and Endogenous Growth," Discussion paper, Mimeo: National University of Singapore.

GOLDMAN, S., AND J. LIGHTWOOD (2002): "Cost Optimization in the SIS Model of Infectious Disease with Treatment," *Topics in Economic Analysis and Policy*, 2(1), 1–22.

GRANDMONT, J.-M. (1986): *On endogenous competitive business cycles*. Springer.

GRASSLY, N., C. FRASER, AND G. GARNETT (2005): "Host immunity and synchronized epidemics of syphilis across the United States," *Nature*, 433, 417–421.

GUO, J.-T., AND A. KRAUSE (2014): "Optimal dynamic nonlinear income taxation under loose commitment," *Macroeconomic Dynamics*, 18(6), 1403–1427.

GUO, J.-T., AND K. J. LANSING (2002): "Fiscal policy, increasing returns, and endogenous fluctuations," *Macroeconomic Dynamics*, 6(5), 633–664.

HETHCOTE, H. W. (2000): "The mathematics of infectious diseases," *SIAM review*, 42(4), 599–653.

HUANG, K. X., AND Q. MENG (2009): "On interest rate policy and equilibrium stability under increasing returns: A note," *Macroeconomic Dynamics*, 13(4), 535–552.

HUANG, K. X., Q. MENG, AND J. XUE (2009): "Is forward-looking inflation targeting destabilizing? The role of policy's response to current output under endogenous investment," *Journal of Economic Dynamics and Control*, 33(2), 409–430.

KAPLAN, E. (1990): "Modeling HIV infectivity: must sex acts be counted?," *JAIDS Journal of Acquired Immune Deficiency Syndromes*, 3(1), 55.

KOROBEINIKOV, A. (2006): "Lyapunov functions and global stability for SIR and SIRS epidemiological models with non-linear transmission," *Bulletin of Mathematical Biology*, 68(3), 615–626.

KOROBEINIKOV, A., AND G. WAKE (2002): "Lyapunov functions and global stability for SIR, SIRS, and SIS epidemiological models," *Applied Mathematics Letters*, 15(8), 955–960.

KREMER, M. (1996): "Integrating behavioral choice into epidemiological models of AIDS," *Quarterly Journal of Economics*, 111(2), 549–573.

LIGHTWOOD, J., AND S. GOLDMAN (1995): "The SIS Model of Infectious Disease with Treatment," Unpublished Manuscript.

OSTER, E. (2005): "Sexually transmitted infections, sexual behavior, and the HIV/AIDS epidemic," *Quarterly Journal of Economics*, 120(2), 467–515.

PHILIPSON, T., AND R. POSNER (1993): *Private Choices and Public Health: The AIDS Epidemic in an Economic Perspective*. Harvard University Press.

ROHANI, P., X. ZHONG, AND A. KING (2010): "Contact network structure explains the changing epidemiology of pertussis," *Science*, 330(6006), 982.

SHIVAMOGGI, B. K. (2014): *Nonlinear dynamics and chaotic phenomena: an introduction*, vol. 103. Springer.

SMITH, B. D. (1989): "Legal restrictions,Şsunspots,Ť and cycles," *Journal of Economic Theory*, 47(2), 369–392.

VAN DEN DRIESSCHE, P., AND J. WATMOUGH (2000): "A simple SIS epidemic model with a backward bifurcation," *Journal of mathematical biology*, 40(6), 525–540.

WOODFORD, M. (1986): "Stationary sunspot equilibria in a finance constrained economy," *Journal of Economic Theory*, 40(1), 128–137.

XIAO, W. (2008): "Increasing Returns and the design of interest rate rules," *Macroeconomic Dynamics*, 12(1), 22.

Appendix A. Derivation of the Economic SIRS Euler Equation with Observable Immunity

Here we derive the Euler equation for the economic SIRS model with observable immunity. To begin, note that equations (9) and (10) imply

$$V_t^R - V_t^{IN} = h + \beta E_t \left[\gamma(V_{t+1}^S - V_{t+1}^R) + (1-v)(V_{t+1}^R - V_{t+1}^{IN}) \right], \tag{A.1}$$

while equations (8) and (9) imply

$$V_t^S - V_t^{IN} = \ln(x_t/\bar{x}) + h + \beta E_t \left[(1-p_t)(V_{t+1}^S - V_{t+1}^{IN}) - v(V_{t+1}^R - V_{t+1}^{IN}) \right]. \tag{A.2}$$

Using equation (11), we have

$$E_t(V_{t+1}^S - V_{t+1}^{IN}) = (\beta x_t p_{x,t})^{-1}, \tag{A.3}$$

for all t. Next, rearrange (A.2) as

$$V_{t+1}^R - V_{t+1}^{IN} = \frac{1}{\beta v}[\ln(x_t/\bar{x}) + h] + \frac{1}{v}(1-p_t)E_t(V_{t+1}^S - V_{t+1}^{IN}) - \frac{1}{\beta v}\left(V_t^S - V_t^{IN}\right). \tag{A.4}$$

Take E_{t-1} on both sides of (A.4) and substitute (A.3) to get

$$E_{t-1}(V_{t+1}^R - V_{t+1}^{IN}) = \frac{1}{\beta v}E_{t-1}[\ln(x_t/\bar{x}) + h] + \frac{1}{\beta v}E_{t-1}\left(\frac{1-p_t}{x_t p_{x,t}}\right) - \frac{1}{\beta^2 v}\left(\frac{1}{x_{t-1}p_{x,t-1}}\right). \tag{A.5}$$

Now rewrite equation (A.1) as

$$V_t^R - V_t^{IN} = h + \beta E_t \left[\gamma(V_{t+1}^S - V_{t+1}^{IN}) + (1 - v - \gamma)(V_{t+1}^R - V_{t+1}^{IN}) \right]. \tag{A.6}$$

Move (A.6) ahead one period, take E_{t-1} of both sides, and set equal to (A.5) to get

$$\frac{1}{\beta v}E_{t-1}\left[\ln(x_t/\bar{x}) + h\right] + \frac{1}{\beta v}E_{t-1}\left(\frac{1-p_t}{x_t p_{x,t}}\right) - \frac{1}{\beta^2 v}\left(\frac{1}{x_{t-1}p_{x,t-1}}\right) \tag{A.7}$$

$$= h + \beta E_{t-1}\left\{ \gamma(\beta x_t p_{x,t})^{-1} + (1 - v - \gamma)\left(\frac{1}{\beta v}\left[\ln(x_t/\bar{x}) + h\right] + \frac{1}{\beta v}\left(\frac{1-p_t}{x_t p_{x,t}}\right) - \frac{1}{\beta^2 v}\left(\frac{1}{x_{t-1}p_{x,t-1}}\right)\right) \right\}.$$

Impose perfect foresight, move ahead one period, and rearrange to get

$$x_t^{-1} = \beta p_{x,t}\left[\ln(x_{t+1}/\bar{x}) + h + \frac{(1 - v - p_{t+1})}{x_{t+1}p_{x,t+1}} - \beta\Delta_{t+2} \right],$$

18

where

$$\Delta_{t+2} = \frac{v\gamma}{x_{t+2}p_{x,t+2}} + (1 - v - \gamma)\left[\ln\left(\frac{x_{t+2}}{\bar{x}}\right) + \frac{1 - p_{t+2}}{x_{t+2}p_{x,t+2}}\right] + (1 - \gamma)\left[h - \frac{1}{\beta x_{t+1}p_{x,t+1}}\right].$$

Appendix B. SIRS Economic Epidemiological (EE) Steady-State and Matrix Systems

Here, we describe the steady state EE system and the linearized EE matrix system used in the bifurcation and stability analyses. The endemic steady states solve time-invariant versions of (6), (7), and the Euler equation. The Euler equation either takes the form of (12) when an indicator variable set at $\phi = 1$ (observable immunity) or the form of (13) when $\phi = 0$ (unobservable immunity). The steady-state system can therefore be rewritten as three equations:

$$in = p(1 - in - r)/(v + \mu) \tag{B.1}$$

$$r = vin/(\gamma + \mu) \tag{B.2}$$

$$x^{-1} = \beta[p_x(\ln(x/\bar{x}) + h - \phi\beta\Delta) + (1 - v - p)/x] \tag{B.3}$$

in three unknown variables (in, r, x), where the immunity externality is given by

$$\Delta = \frac{1}{p_x x}[v\gamma + (1 - v - \gamma)(1 - p) - (1 - \gamma)/\beta] + (1 - v - \gamma)\ln(x/\bar{x}) + (1 - \gamma)h.$$

Similar to Goenka, Liu, and Nguyen (2012), we also note the existence of an eradication steady and focus on the local stability properties around the endemic steady states.

To analyze these transition dynamics, we linearize around the endemic steady states:

$$\widehat{in}_{t+1} = (1 - v - \mu - p)\widehat{in}_t + (1 - in - r)\hat{p}_t - p\hat{r}_t \tag{B.4}$$

$$\hat{r}_{t+1} = (1 - \gamma - \mu)\hat{r}_t + v\widehat{in}_t, \tag{B.5}$$

where hats (ˆ) over the variables indicate deviation from one of the steady states. The linearized Euler equation is:

$$p_x\hat{x}_t + x\hat{p}_{x,t} = \beta p_x(1 - v - p - xp_x)E_t\hat{x}_{t+1} + \beta x(1 - v - p)E_t\hat{p}_{x,t+1} + \beta xp_x E_t\hat{p}_{t+1} \quad \text{(B.6)}$$

$$+\phi\beta^2 E_t \left\{ \begin{array}{l} p_x[v\gamma + (1 - v - \gamma)(1 - p - xp_x)]\hat{x}_{t+2} + x[v\gamma + (1 - v - \gamma)(1 - p)]\hat{p}_{x,t+2} + \\[2mm] [(1 - v - \gamma)xp_x]\hat{p}_{t+2} - [(1 - \gamma)p_x/\beta]\hat{x}_{t+1} - [(1 - \gamma)x/\beta]\hat{p}_{x,t+1} \end{array} \right\}$$

where

$$\hat{p}_t = p_{in}\widehat{in}_t + p_x\hat{x}_t \quad \text{(B.7)}$$

$$\hat{p}_{x,t} = [(1 + \ln[1 - p])/x]\hat{p}_t - (p_x/x)\hat{x}_t \quad \text{(B.8)}$$

and

$$p_{in} = x\lambda(1 - \lambda in)^{x-1} \quad \text{(B.9)}$$

$$p_x = -\ln(1 - p)(1 - p)/x. \quad \text{(B.10)}$$

In matrix form, the EE system can be written as

$$\hat{z}_t = J\,\hat{z}_{t+1}, \quad \text{(B.11)}$$

where $\hat{z}_t = (\hat{x}_t, \widehat{in}_t, \hat{r}_t)'$ when $\phi = 0$ or $\hat{z}_t = (\hat{x}_t, \widehat{in}_t, \hat{r}_t, \hat{x}_{t+1}, \widehat{in}_{t+1})'$ when $\phi = 1$, and J is the transition matrix.

Specifically, if we impose perfect foresight, the $\phi = 0$ linearized EE matrix system can be written as:

$$\underbrace{\begin{bmatrix} 0 & 1 - v - \mu - p & -p \\ 0 & v & 1 - \gamma - \mu \\ p_x & 0 & 0 \end{bmatrix}}_{A} \begin{bmatrix} \hat{x}_t \\ \widehat{in}_t \\ \hat{r}_t \end{bmatrix} + \underbrace{\begin{bmatrix} 1 - in - r & 0 \\ 0 & 0 \\ 0 & x \end{bmatrix}}_{B} \begin{bmatrix} \hat{p}_t \\ \hat{p}_{x,t} \end{bmatrix}$$

$$= \underbrace{\begin{bmatrix} 0 & 1 & 0 \\ 0 & 0 & 1 \\ \beta p_x(1 - v - p - xp_x) & 0 & 0 \end{bmatrix}}_{C} \begin{bmatrix} \hat{x}_{t+1} \\ \widehat{in}_{t+1} \\ \hat{r}_{t+1} \end{bmatrix} + \underbrace{\begin{bmatrix} 0 & 0 \\ 0 & 0 \\ \beta xp_x & \beta x(1 - v - p) \end{bmatrix}}_{D} \begin{bmatrix} \hat{p}_{t+1} \\ \hat{p}_{x,t+1} \end{bmatrix} \quad \text{(B.12)}$$

and

$$\underbrace{\begin{bmatrix} -1 & 0 \\ -(1+\ln(1-p))/x & 1 \end{bmatrix}}_{F} \begin{bmatrix} \hat{p}_t \\ \hat{p}_{x,t} \end{bmatrix} = -\underbrace{\begin{bmatrix} p_x & p_{in} & 0 \\ p_x/x & 0 & 0 \end{bmatrix}}_{G} \begin{bmatrix} \hat{x}_t \\ \widehat{in}_t \\ \hat{r}_t \end{bmatrix}. \tag{B.13}$$

When $\phi = 1$, we have

$$\underbrace{\begin{bmatrix} 0 & 1-v-\mu-p & -p & 0 & 0 \\ 0 & v & 1-\mu-\gamma & 0 & 0 \\ p_x & 0 & 0 & 0 & 0 \\ 0 & 0 & 0 & 1 & 0 \\ 0 & 0 & 0 & 0 & 1 \end{bmatrix}}_{A} \begin{bmatrix} \hat{x}_t \\ \widehat{in}_t \\ \hat{r}_t \\ \hat{x}_{t+1} \\ \widehat{in}_{t+1} \end{bmatrix} + \underbrace{\begin{bmatrix} s & 0 & 0 & 0 \\ 0 & 0 & 0 & 0 \\ 0 & x & 0 & 0 \\ 0 & 0 & 0 & 0 \\ 0 & 0 & 0 & 0 \end{bmatrix}}_{B} \begin{bmatrix} \hat{p}_t \\ \hat{p}_{x,t} \\ \hat{p}_{t+1} \\ \hat{p}_{x,t+1} \end{bmatrix}$$

$$= \underbrace{\begin{bmatrix} 0 & 1 & 0 & 0 & 0 \\ 0 & 0 & 1 & 0 & 0 \\ \beta p_x(1-v-p-xp_x)-\beta^2[(1-\gamma)p_x/\beta] & 0 & 0 & \beta^2 p_x[v\gamma+(1-v-\gamma)(1-p-xp_x)] & 0 \\ 1 & 0 & 0 & 0 & 0 \\ 0 & 1 & 0 & 0 & 0 \end{bmatrix}}_{C} \begin{bmatrix} \hat{x}_{t+1} \\ \widehat{in}_{t+1} \\ \hat{r}_{t+1} \\ \hat{x}_{t+2} \\ \widehat{in}_{t+2} \end{bmatrix} +$$

$$\underbrace{\begin{bmatrix} 0 & 0 & 0 & 0 \\ 0 & 0 & 0 & 0 \\ \beta xp_x & \beta x(1-v-p)-\beta^2[(1-\gamma)x/\beta] & \beta^2(1-v-\gamma)xp_x & \beta^2 x[v\gamma+(1-v-\gamma)(1-p)] \\ 0 & 0 & 0 & 0 \\ 0 & 0 & 0 & 0 \end{bmatrix}}_{D} \begin{bmatrix} \hat{p}_{t+1} \\ \hat{p}_{x,t+1} \\ \hat{p}_{t+2} \\ \hat{p}_{x,t+2} \end{bmatrix}$$

and

$$\underbrace{\begin{bmatrix} -1 & 0 & 0 & 0 \\ -(1+\ln(1-p))/x & 1 & 0 & 0 \\ 0 & 0 & -1 & 0 \\ 0 & 0 & -(1+\ln(1-p))/x & 1 \end{bmatrix}}_{F} \begin{bmatrix} \hat{p}_t \\ \hat{p}_{x,t} \\ \hat{p}_{t+1} \\ \hat{p}_{x,t+1} \end{bmatrix} = -\underbrace{\begin{bmatrix} p_x & p_{in} & 0 & 0 & 0 \\ p_x/x & 0 & 0 & 0 & 0 \\ 0 & 0 & 0 & p_x & p_{in} \\ 0 & 0 & 0 & p_x/x & 0 \end{bmatrix}}_{G} \begin{bmatrix} \hat{x}_t \\ \widehat{in}_t \\ \hat{r}_t \\ \hat{x}_{t+1} \\ \widehat{in}_{t+1} \end{bmatrix}. \tag{B.14}$$

where

$$J = (A - BF^{-1}G)^{-1}(C - DF^{-1}G). \tag{B.15}$$

We use the method of Blanchard and Kahn (1980) to analyze the nature of the rational expectation EE equilibrium. When $\phi = 0$ the three-variable system contains one jump ($\hat{x}_t$) and two predetermined ($\widehat{in}_t$ and $\hat{r}_t$) variables. The system will exhibit saddle-path stability if there are two eigenvalues of J outside the unit circle, indeterminate multiple stable paths if there are no forward stable eigenvalues, and explosive paths if there is more than one forward-stable eigenvalue. When $\phi = 1$ the five-variable system contains three jump ($\hat{x}_t$, $\hat{x}_{t+1}$ and $\widehat{in}_{t+1}$) and two predetermined ($\widehat{in}_t$ and $\hat{r}_t$) variables. The fifth equation is an identity for $\widehat{in}_{t+1}$ with a zero eigenvalue. Considering the other four eigenvalues, the system will exhibit saddle-path stability if exactly two of the eigenvalues are outside the unit circle, indeterminate multiple stable paths if there are three or more eigenvalues outside the unit circle, and explosive paths if there is less than two eigenvalues outside the unit circle.

Figure 1. Optimal Choices and Bifurcation for the Economic SIS Model
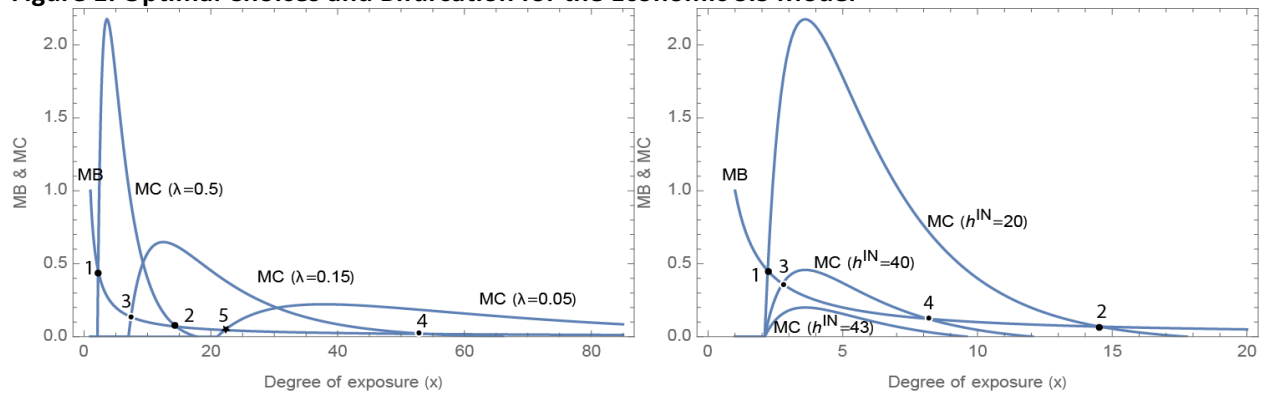
(a) Optimal Choices
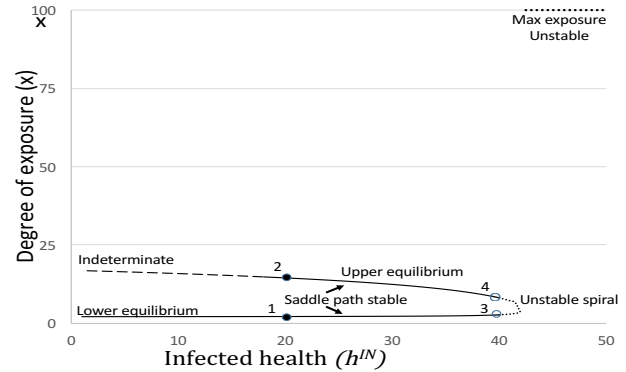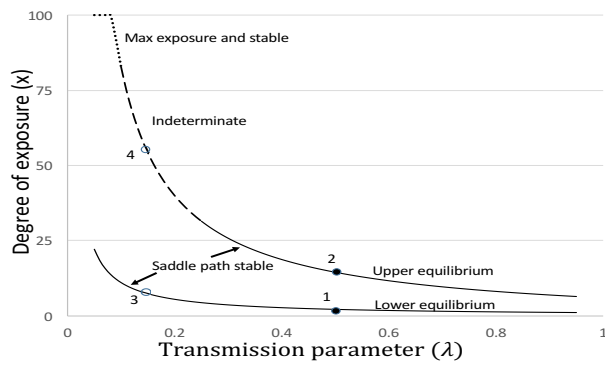
(b) Bifurcation in degree of exposure
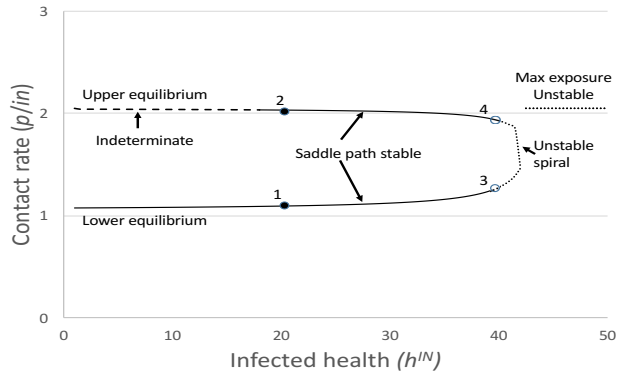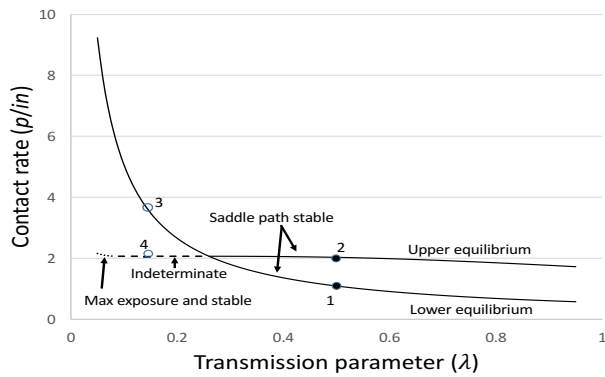
(c) Bifurcation in contact rate
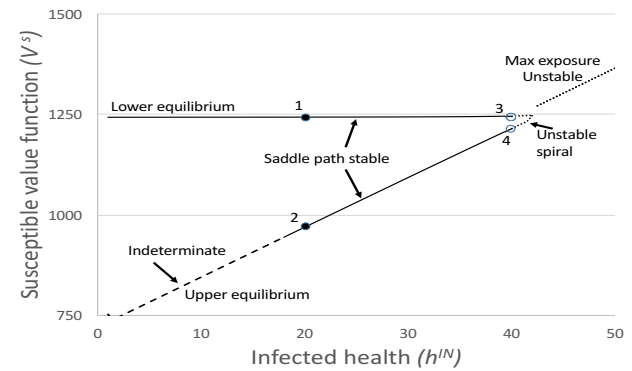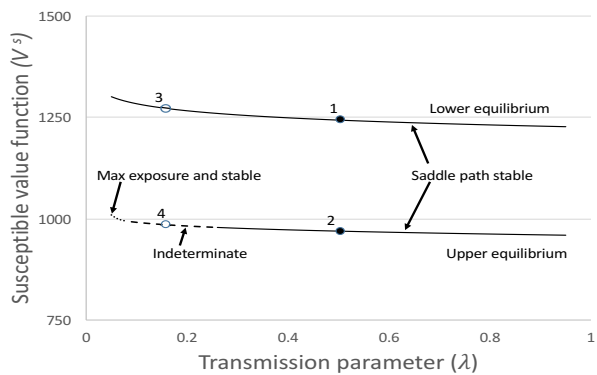
(d) Bifurcation in susceptible value function

Figure 2. Nonlinear Transition Dynamics
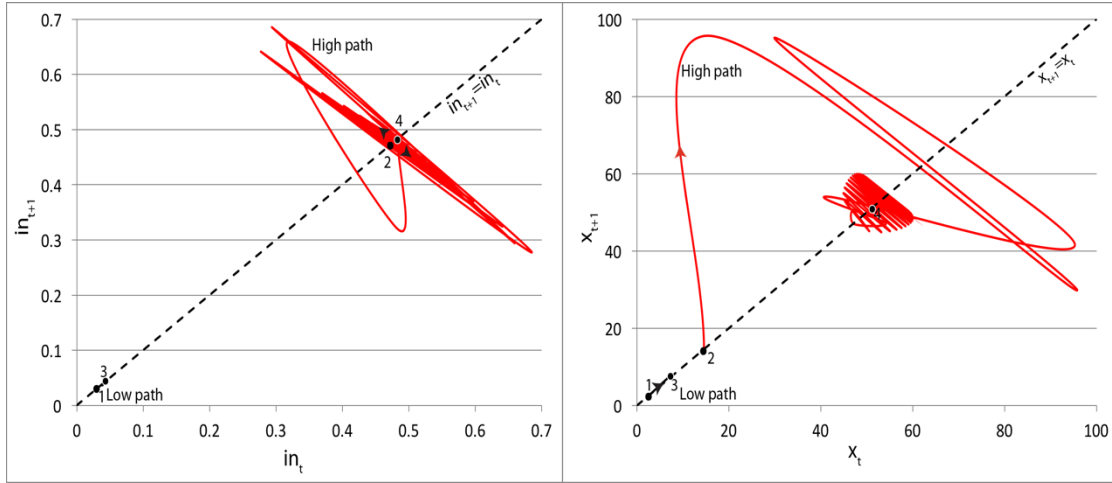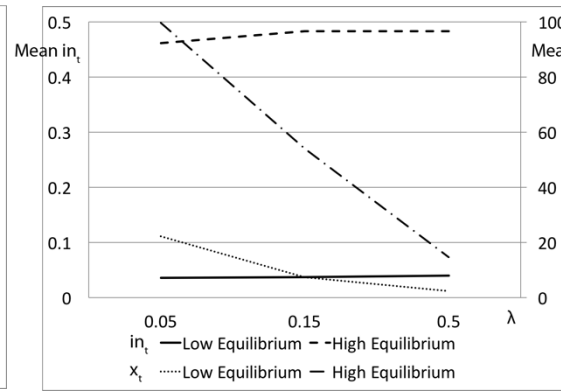

(a) Paths from reduction to $\lambda = 0.15$
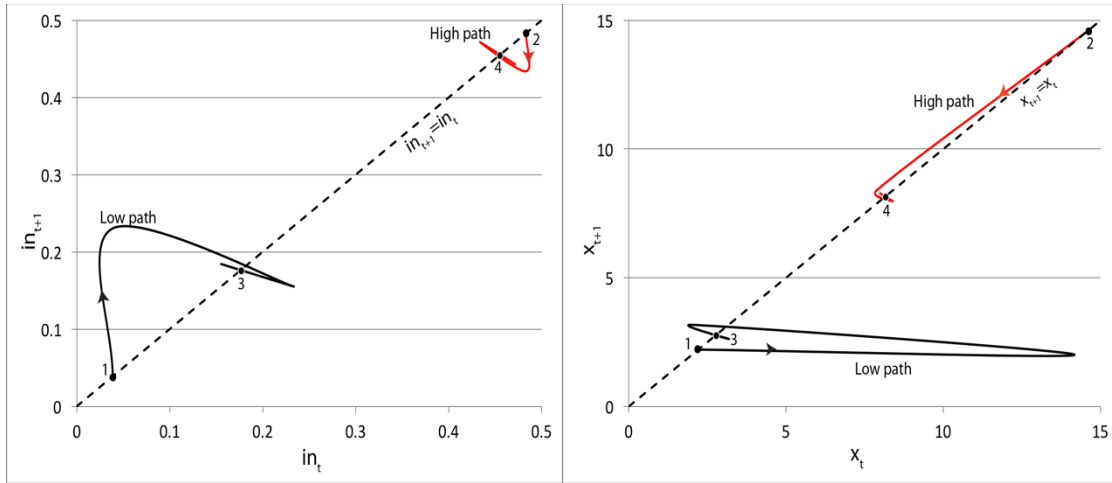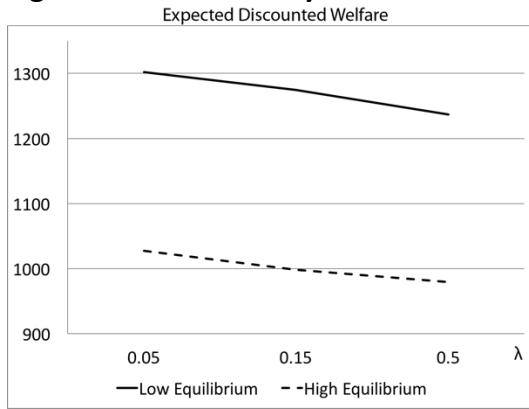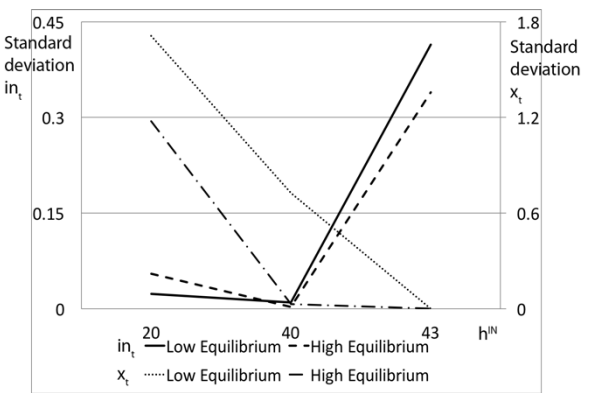

(b) Paths from increase $h^{IN} = 40$
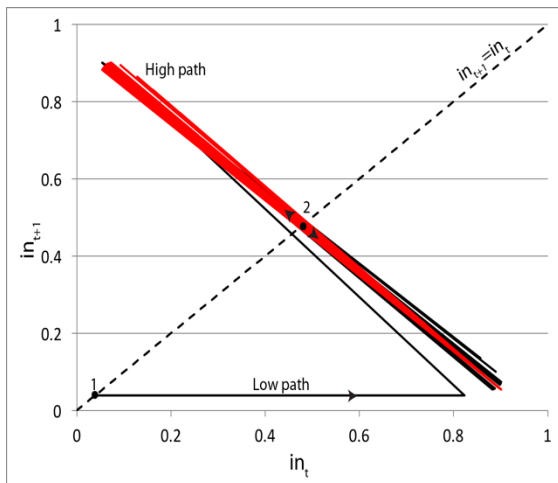
(c) Paths from increase to $h^{IN} = 43$ (exposure at upper bound)

Figure 3. Welfare Analysis
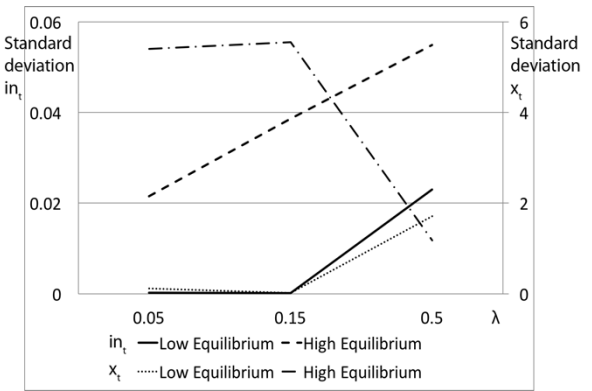
(a) Changes in λ
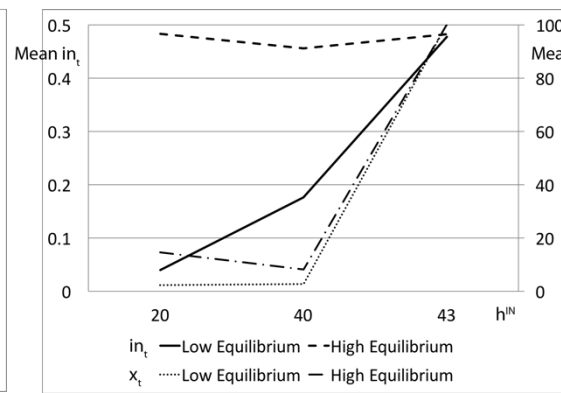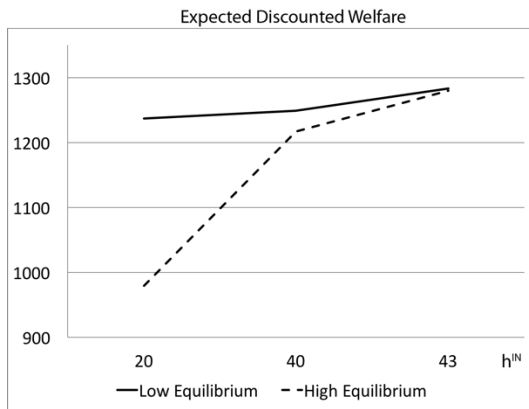
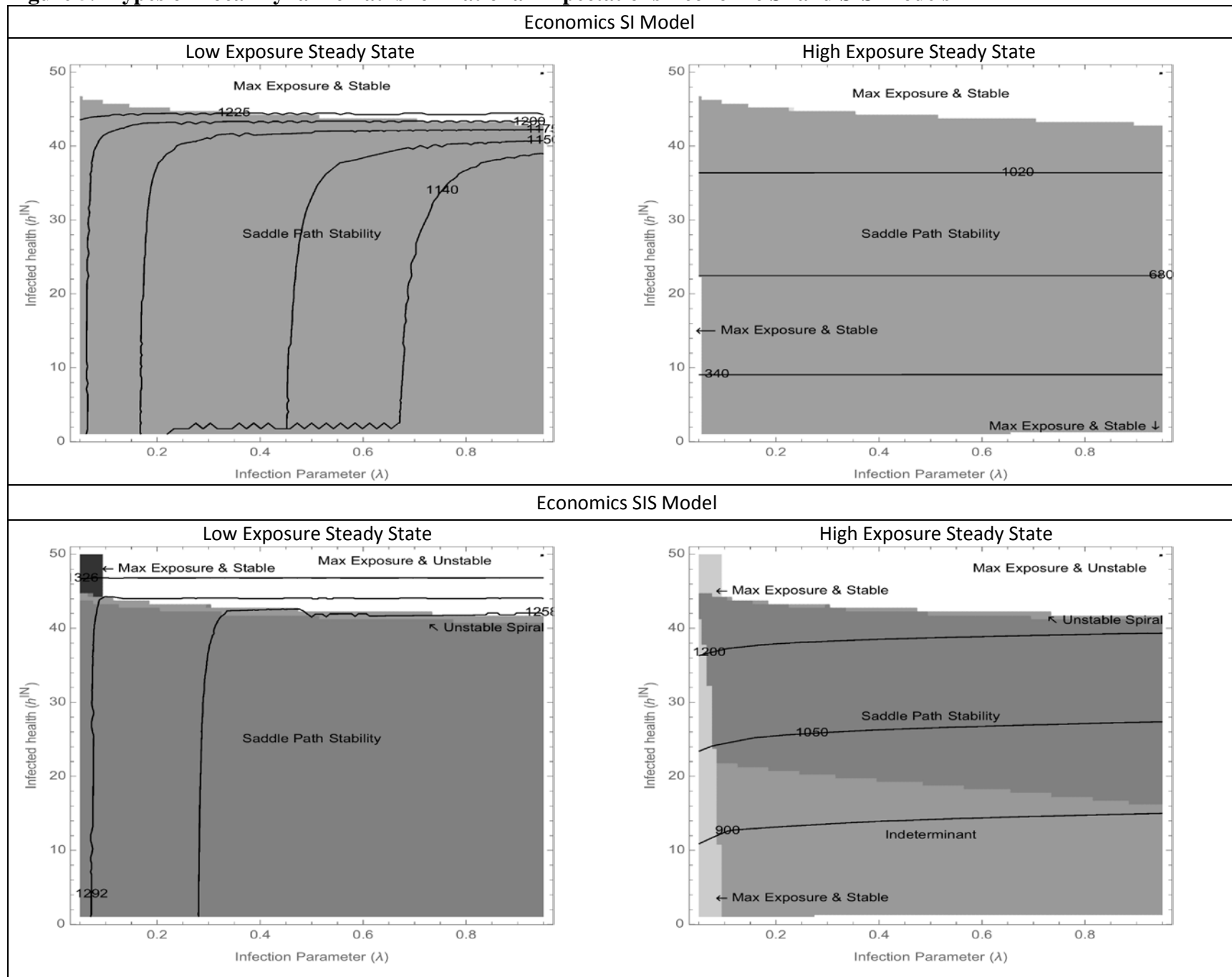**(b)** Changes in h^{IN}
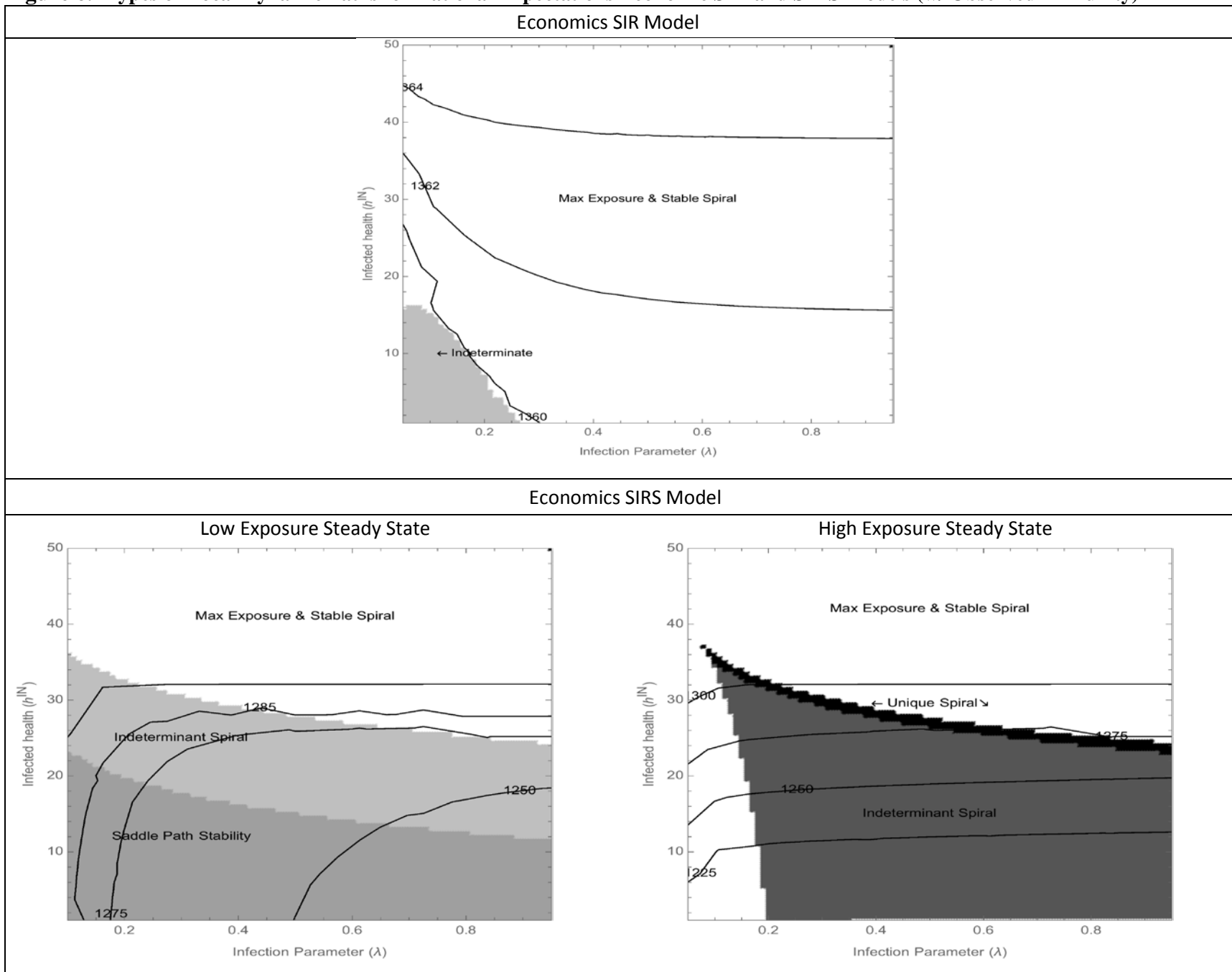
Figure 4. Immunity Externality
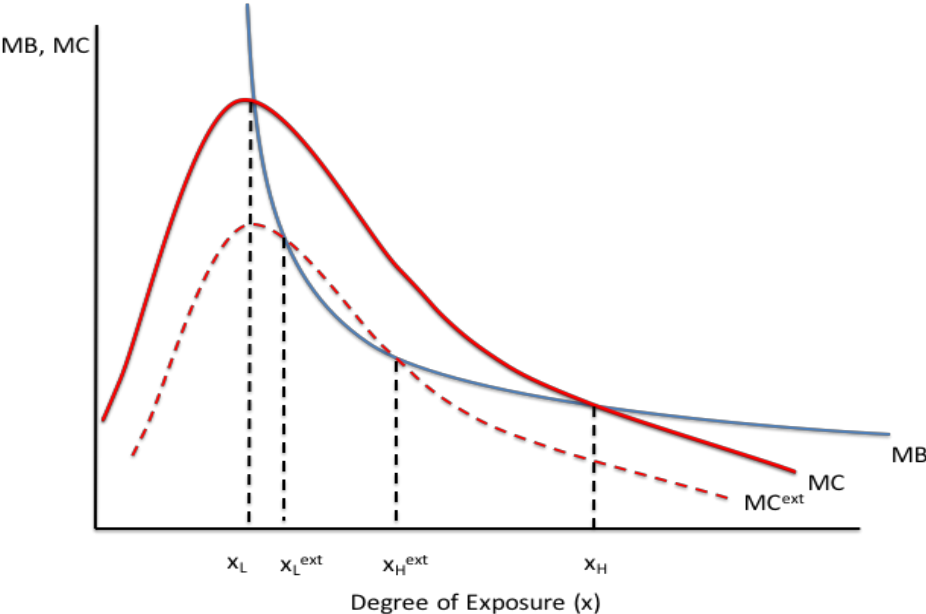
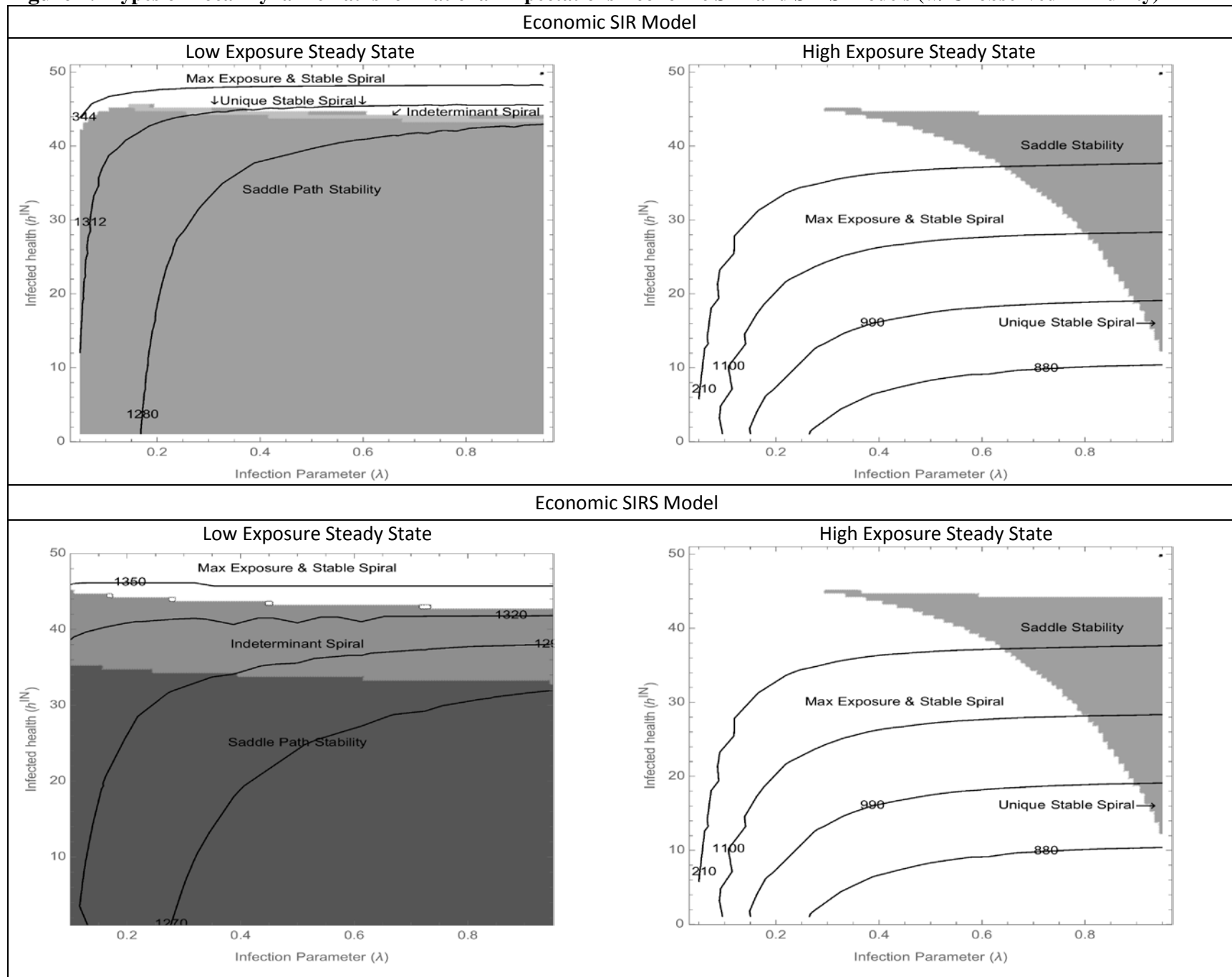**Figure 5. Types of Local Dynamic Paths for Rational Expectations Economic SI and SIS Models**

Notes: Contour lines indicate welfare at the steady state. Parameter values are given in Table 1.

Figure 6. Types of Local Dynamic Paths for Rational Expectations Economic SIR and SIRS Models (w/ Observed Immunity)

Notes: Contour lines indicate welfare at the steady state. Parameter values are given in Table 1.

Figure 7. Types of Local Dynamic Paths for Rational Expectations Economic SIR and SIRS Models (w/ Unobserved Immunity)

Notes: Contour lines indicate welfare at the steady state. Parameter values are given in Table 1.